Research Article

MOLECULAR PAIN

Molecular Pain
Volume 16: 1–13

DOI: 10.1177/1744806920915339
journals.sagepub.com/home/mpx
SAGE

Group II metabotropic glutamate receptor expressing neurons in anterior cingulate cortex become sensitized after inflammatory and neuropathic pain

Sisi Chen[1], Feni Kadakia[2], and Steve Davidson[1,2]

Abstract

The anterior cingulate cortex is a limbic region associated with the emotional processing of pain. How neuropathic and inflammatory pain models alter the neurophysiology of specific subsets of neurons in the anterior cingulate cortex remains incompletely understood. Here, we used a *GRM2*^{Cre}:tdtomato reporter mouse line to identify a population of pyramidal neurons selectively localized to layer II/III of the murine anterior cingulate cortex. *GRM2* encodes the group II metabotropic glutamate receptor subtype 2 which possesses analgesic properties in mouse and human models, although its function in the anterior cingulate cortex is not known. The majority of *GRM2*-tdtomato anterior cingulate cortex neurons expressed *GRM2* gene product in situ but did not overlap with cortical markers of local inhibitory interneurons, parvalbumin or somatostatin. Physiological properties of *GRM2*-tdtomato anterior cingulate cortex neurons were investigated using whole-cell patch clamp techniques in slice from animals with neuropathic or inflammatory pain, and controls. After hind-paw injection of Complete Freund's Adjuvant or chronic constriction injury, *GRM2*-tdtomato anterior cingulate cortex neurons exhibited enhanced excitability as measured by an increase in the number of evoked action potentials and a decreased rheobase. This hyperexcitability was reversed pharmacologically by bath application of the metabotropic glutamate receptor subtype 2 agonist (2R, 4R)-4-Aminopyrrolidine-2,4-dicarboxylate APDC (1 μM) in both inflammatory and neuropathic models. We conclude that layer II/III pyramidal *GRM2*-tdtomato anterior cingulate cortex neurons express functional group II metabotropic glutamate receptors and undergo changes to membrane biophysical properties under conditions of inflammatory and neuropathic pain.

Keywords

Anterior cingulate cortex, metabotropic glutamate receptor, inflammatory, neuropathic, pain, group II

Date Received: 23 July 2019; Revised 27 January 2020; accepted: 7 February 2020

Introduction

Chronic pain, often a result of tissue inflammation or nerve damage, is a major cause of reduced quality of life. Many strategies for pain management are inadequate or include opioid drugs with unwanted side-effects and a high potential for abuse. Deficiencies in pain management can generate or exacerbate comorbidities such as stress, anxiety, and depression, underscoring the common and complex relationship between somatosensory homeostasis and psychiatric disorders.[1–3] Functional neural plasticity and neuroanatomical changes within the brain, far from the site of injury, have been suggested to contribute to the chronification and maintenance of pain.[4] For example, cortical hyperactivity initially induced by peripheral nerve injury was not suppressed even after peripheral injury-evoked signals were blocked.[5] Such ongoing, higher order central

[1]Department of Anesthesiology, Pain Research Center, University of Cincinnati College of Medicine, Cincinnati, OH, USA
[2]Neuroscience Graduate Program, University of Cincinnati College of Medicine, Cincinnati, OH, USA

Corresponding Author:
Steve Davidson, Department of Anesthesiology, University of Cincinnati College of Medicine, Cincinnati, OH, USA.
Email: steve.davidson@uc.edu

sensitization, particularly within limbic areas, is well positioned to contribute to ongoing affective and motivational dimensions of pain and may facilitate the psychiatric comorbidity.[6]

The anterior cingulate cortex (ACC) has emerged as a primary site for pain and emotional processing; it is activated during noxious somatosensory stimulation and its activity and neuroanatomy become reorganized in patients with chronic pain.[7–10] Animal models of pain produce altered neural excitability and synaptic plasticity in the ACC including long-term potentiation or depression mediated by ionotropic glutamatergic signaling.[11] Glutamatergic signaling in ACC has been critically and specifically linked to affective pain processing.[12–14] Metabotropic glutamate receptors (mGluRs) have also been implicated in ACC signaling related to pain, in particular, group I mGluRs (mGluR1/5) have been shown to have a facilitatory role in nociception.[15–17]

In contrast, group II mGluRs, encoded by *GRM2* and *GRM3*, canonically couple to the $G_{i/o}$ intracellular signaling pathway to suppress cyclic adenosine monophosphate (cAMP) and neural excitability.[18] We previously showed that activation of group II mGluRs suppressed hyperexcitability in both mouse and human nociceptors in vitro.[19] Group II mGluRs are also expressed in the brain,[20–22] and systemic group II mGluR agonist administration produces antinociceptive behavioral effects, raising the possibility that group II mGluRs may be capable modulating pain supraspinally.[23,24] Indeed, activation of group II mGluRs in medial prefrontal cortex (mPFC) and the amygdala had modulatory effects on an arthritic pain model.[25–28] Recently, group II mGluRs were shown to modulate excitatory neurotransmission in human cortical neurons.[29] However, much remains unknown regarding the identity of the group II mGluR expressing neurons within the forebrain. Small molecule modulators of group II mGluRs are currently in clinical trials for nonpain disorders, but may be a potential tool for pain management, underscoring the need to understand the functional roles of group II mGluR expressing neurons. Here, we report on a transgenic murine model to identify *GRM2* ACC neurons in the mouse and investigate the anatomy and membrane physiology of this population under inflammatory and neuropathic pain conditions.

Materials and methods

Animals

Both male and female mice (8–12 weeks of age) were included in the study. *GRM2*^{Cre} mice were generated on a C57BL/6j background from cryo-preserved sperm (stock number: 036166-UCD; Strain Name: Tg(*Grm2*-cre)MR89Gsat/Mmucd) from the Mutant Mouse Resource and Research Center at UC Davis. Ai9 (ROSA26$^{LSL\text{-}tdtomato}$) mice were purchased from Jackson Labs. The *GRM2*^{Cre} line was crossed with the Ai9 line to obtain offspring that expressed tdtomato fluorescent protein in *GRM2* neurons. The experimental protocols were approved by the Institutional Animal Care and Use Committee of the University of Cincinnati and conducted in accordance with the National Institutes of Health Guide for the Care and Use of Laboratory Animals. Mice were housed four per cage at 22 ± 0.5°C under a controlled diurnal cycle of 12 h light and 12 h dark, with food and water ad libitum.

Histology, immunohistochemistry, and in situ hybridization

To obtain brain tissues, mice were first anesthetized with isoflurane, then perfused with 0.01 M phosphate buffer, followed by perfusion with 4% paraformaldehyde (PFA). Brains were extracted and placed in 4% PFA for 2 h at room temperature (RT), followed by transfer to 30% sucrose at 4°C. Frozen sections were cut at 30 µm using a Leica CM1860 UV cryostat (Leica Biosystems Inc., Buffalo Grove, IL, USA). For histology, specimens were washed with 0.01M phosphate buffer, dried, and coverslipped for microscopy. For immunohistochemistry, antiparvalbumin primary antibody (PV, rabbit polyclonal Ab, 1:100, Invitrogen, catalog# PA1-933) and secondary antibody (Donkey anti rabbit, 1:1000, Alexa Fluor 488, Thermo-Fisher, catalog# A21206) and antisomatostatin (rat monoclonal Ab, 1:50, Abcam, catalog# 30788) and secondary antibody (Donkey anti Rat, 1:1000, Alexa Fluor 488, catalog# A-21208) were used. To assess the morphological properties of *GRM2*-tdtomato neurons, biocytin (Invitrogen, catalog# B1592) was delivered from the recording pipette which was left in place for another 20 min after recordings were done. Brain slices obtained after electrophysiology were fixed in 4% PFA for at least 30 min at RT and then incubated in Alexa Fluor 488 streptavidin (1:300, Invitrogen, catalog# 32354) in 1% Triton-X 100 phosphate-buffered saline overnight at 4°C. For in situ *hybridization* using RNAscope, 2 *GRM2*^{Cre}; ROSA26$^{LSL\text{-}tdtomato}$ mice were anesthetized and perfused, followed by transfer to RNAse-free 30% sucrose overnight. Frozen sections were cut at 14 µm and then stored at −80°C. RNAscope Multiplex Fluorescent v2 Assay (Advanced Cell Diagnostics Inc., Newark, CA, USA) was carried out for fresh-frozen tissue as recommended by the manufacturer. The RNAscope Mm-*GRM2* (#108068) probe was hybridized and developed with a single channel. Tyramide Signal Amplification (TSA) Plus Cyanine 5 systems (1:1000, PerkinElmer) was diluted with TSA buffer to visualize the *GRM2*

hybridized signal. Slides were counterstained with 4',6-diamidino-2-phenylindole (DAPI) and coverslipped with Prolong Gold Antifade Reagent (Invitrogen). Image acquisition was captured as Z stacks with an Olympus BX63 epifluorescence microscope using CellSens Dimension Desktop software (Olympus). Cells containing three or more fluorescent puncta were considered to be positive.

Hind-paw inflammation with Complete Freund's Adjuvant

Under manual restraint, Complete Freund's Adjuvant (CFA) (10 µL, Thermo-Fisher, catalog# 77140) was injected subcutaneously into the plantar left hind paw using a 31 gauge needle (BD, Franklin Lakes, NJ, USA).[30] Mice were returned to their home cage for 24 h before further experiments.

Chronic constriction injury model

A peripheral mononeuropathy was produced by loosely ligating the sciatic nerve using methodology adapted from Bennet and Xie.[31] Briefly, under isoflurane anesthesia, the left sciatic nerve was exposed at mid-thigh level by blunt dissection through the biceps femoris muscle. Three loosely constrictive ligatures (6–0 chromic gut suture; ETHICON, Somerville, NJ, USA) were tied around the sciatic nerve with at least 0.5 mm between sutures. Muscle and skin were sutured closed in layers. Sham operations exposed and freed the nerve, but no ligatures were used. Mice were returned to their home cage for seven days before further experiments.

Brain slice preparation

Mice were deeply anesthetized with isoflurane and perfused with 20 to 30 mL ice-cold carbogenated (95% O_2, 5% CO_2) N-Methyl-D-glucamine (NMDG)-artificial cerebrospinal fluid (aCSF) (in mM: 92 NMDG, 2.5 KCl, 1.25 NaH_2PO_4, 30 $NaHCO_3$, 20 4-(2-Hydroxyethyl)piperazine-1-ethanesulfonic acid (HEPES), 25 glucose, 2 thiourea, 5 Na-ascorbate, 3 Na-pyruvate, 0.5 $CaCl_2{\cdot}4H_2O$, and 10 $MgSO_4{\cdot}7H_2O$), 300 to 310 mOsm adjusted with sucrose, pH 7.4 with adjusted with HCl. Mice were then decapitated, and brains were quickly extracted into NMDG-aCSF solution then glued onto a mounting cylinder. Brains were cut at a thickness of 300 µm using a VF-300-0z compresstome (Precisionary Instruments, Greenville, NC, USA). Brain slices (between approximately +1.2 mm and 0 mm Bregma) were then incubated for recovery in NMDG-aCSF solution for 15 min at RT. Slices were transferred into RT aCSF-HEPES (in mM: 92 NaCl, 2.5 KCl, 1.25 NaH_2PO_4, 30 $NaHCO_3$, 20 HEPES, 25 glucose, 2 thiourea, 5 Na-ascorbate, 3 Na-pyruvate, 2 $CaCl_2{\cdot}4H_2O$, and 2 $MgSO_4{\cdot}7H_2O$, 300–310 mOsm adjusted with sucrose, pH 7.4) prior to recording.

Electrophysiology

Brain slices were transferred to a recording chamber and secured using a slice anchor under the objective of an upright microscope (Olympus BX51). All recordings were performed from the right, contralateral hemisphere with continuous whole-bath perfusion, with a flow rate at 1 to 2 mL/min and temperature was maintained at 32°C using a dual automatic temperature controller (TC-344C, Warner Instruments) monitored with a feedback thermistor positioned in the bath. The slice was visualized with an infrared light source and video camera (Rolera Bolt). For fluorescent detection of tdtomato-expressing neurons, LED illumination (CoolLED, p-4000) with Texas Red filter cube was used. Whole-cell recordings were performed in extracellular bath solution containing (in mM) 145 NaCl, 3 KCl, 2.5 $CaCl_2$, 1.2 $MgCl_2$, 10 HEPES, 7 glucose, adjusted to pH 7.4 with NaOH. Patch pipettes were pulled from standard-walled, filamented 1.5/0.86 OD/ID (outer diameter/inner diameter) borosilicate glass (Warner Instruments, Hamden, NJ, USA), with open tip resistances ranging from 4 to 6 MΩ using a P-1000 micropipette puller (Sutter Instrument, Novato, CA, USA). For experiments testing membrane properties in current clamp, the intracellular solution contained (in mM) 130 K-gluconate, 5 KCl, 5 NaCl, 2 $MgCl_2$, 0.3 Ethelyene glycol-bis(2-aminoethylether)-NNN'N'-tetra-acetic acid (EGTA), 10 HEPES, 2 Na ATP, adjusted to pH 7.3 with KOH and 294 mOsm with sucrose, with biocytin added (3–5 mg/mL). After whole-cell access and adjusting the capacitance, neurons were held at −70 mV for a minimum of 2 min before recording. Neurons with resting membrane potential > -45 mV were not studied further. Recordings were obtained on a MultiClamp 700B and sampled at 20 kHz and filtered at 10 kHz using a Digidata 1550 A (Molecular Devices). Data were collected and analyzed with Clampex 10.5 and Clampfit 10.5 software (Molecular Devices). The group II mGluR agonist 2R, 4R-(2R, 4R)-4-Aminopyrrolidine-2,4-dicarboxylate (APDC) (1 µM; Tocris) was dissolved in external solution using a gravity-fed perfusion system (Harvard apparatus). All membrane properties (rheobase, max dv/dt, threshold, action potential height/width, tau, after hyperpolarization, and input resistance) were assessed on the first evoked action potential elicited from an 800 ms square pulse of increasing magnitude (20 pA/step). Tau was calculated from peak after-hyperpolarization (AHP) to 90% depolarization to baseline.

Statistical analysis

All statistical analyses were performed using GraphPad Prism (San Diego, CA, USA). For *GRM2*-tdtomato neuron membrane biophysics and action potential properties analyses, one-way analysis of variance (ANOVA) was used to determine the difference among groups. For *GRM2*-tdtomato neuron firing frequency analysis, two-way ANOVA with Sidak's post hoc test was used to compare between groups. Fisher's exact test was used to compare proportional data. Unpaired Student's t tests were used to compare two groups. For all statistical analyses, significance was defined as $p < 0.05$. Data are presented as mean ± standard error of the mean. *$p < 0.05$; **$p < 0.01$; ***$p < 0.001$; ****$p < 0.0001$. N values are number of cells recorded.

Results

GRM2-tdtomato ACC neurons are pyramidal and located predominantly in layer II/III

Transgenic reporter mice *GRM2*^{Cre}; ROSA26$^{LSL\text{-}tdtomato}$ were used to identify *GRM2*-postive neurons in the ACC (*GRM2*-tdtomato). *GRM2*-tdtomato somata were located at least 120 μm from the brain surface at the longitudinal fissure, and the majority of neurons occupied a band extending to a depth of approximately 300 μm in ACC (Figure 1(a) and (b)). These observations are consistent with previous observations from immunohistological and in situ reports of metabotropic glutamate receptor subtype 2 (mGluR2)/*GRM2*[22,32] (see also: GENSAT Brain Atlas, MR89-Cre). The band of *GRM2*-tdtomato neurons was present in both Cg1 and Cg2 and were observed to be most densely localized within layer II/III,[33] although a smaller number of tdtomato-labeled cells were also observed in deeper layers. To assess the morphology of individual *GRM2*-tdtomato neurons, biocytin was used to visualize neuronal somata and neurite extensions after recording (Figure 1(c)). *GRM2*-tdtomato neurons in layer II/III ACC were identified as pyramidal type with somatic dendrites extending 100 to 150 μm in a radial pattern and an apical dendrite which seldom branched until reaching layer I. To determine whether the fluorescent signal in *GRM2*-tdtomato neurons corresponds to ongoing *GRM2* gene expression, in situ hybridization with

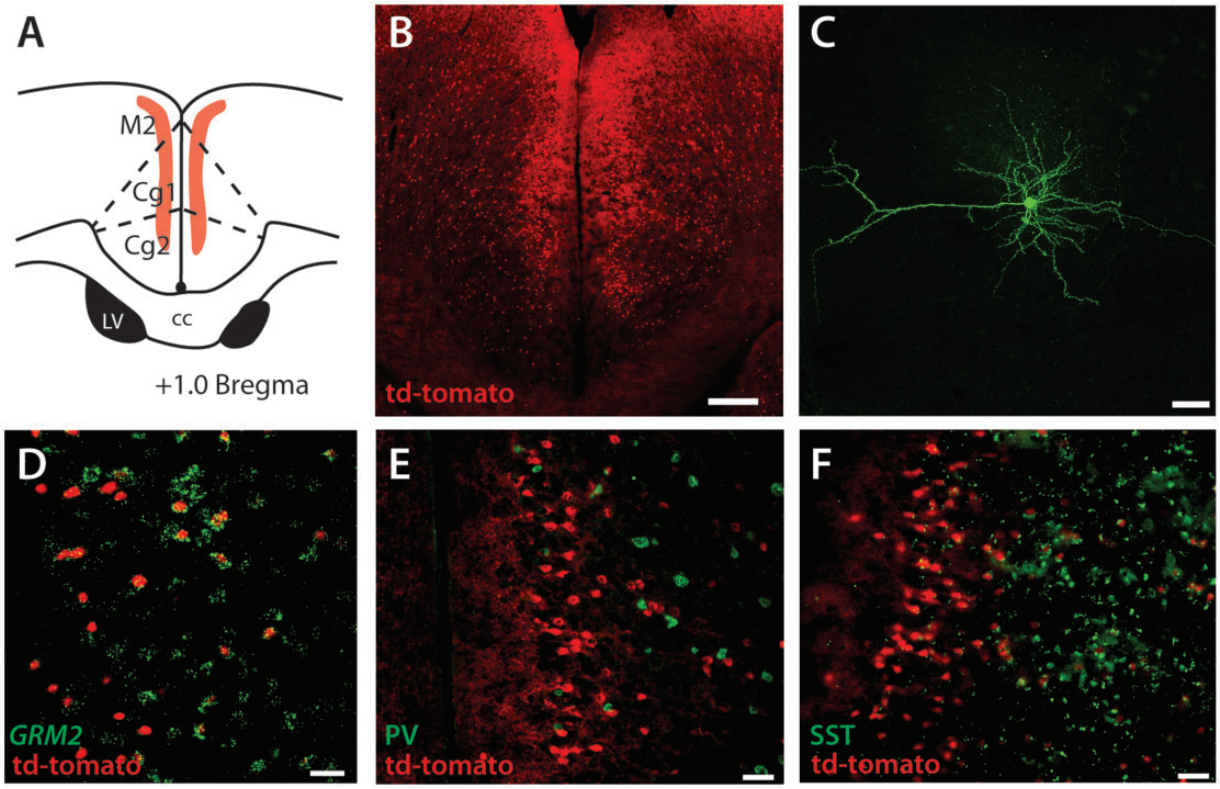

Figure 1. *GRM2*-tdtomato expression in ACC is localized to layer II/III pyramidal neurons. (a) Schematic of ACC area under investigation in this study. (b) *GRM2*^{Cre}; ROSA26$^{LSL\text{-}tdtomato}$ mouse expresses red fluorescent protein in layer II/III in ACC. Scale bar = 200 μm. (c) Biocytin labeling of *GRM2*-tdtomato neurons in layer II/III ACC, which were all pyramidal and send apical dendrites to layer I. Scale bars = 50 μm. (d) RNAscope in situ histochemistry of *GRM2*. (e) Immunohistochemistry shows lack of overlap of ACC *GRM2*-tdtomato neurons with PV or SST (f), Scale bars = 100 μm. PV: parvalbumin; SST: somatostatin.

RNAscope was performed to test colocalization. We observed that 78% of *GRM2*-tdtomato neurons also expressed *GRM2* in situ hybridization signal (Figure 1 (d)). The in situ signal often surrounded or encapsulated the cytosolic *GRM2*-tdtomato expression. In situ signal for *GRM2* was also observed unassociated with tdtomato somata, suggesting that tdtomato may not be expressed in all *GRM2* expressing somata in this transgenic model. Colocalization experiments with immunohistochemical markers of cortical interneurons showed that *GRM2*-tdtomato neurons did not overlap with parvalbumin or somatostatin expressing neurons in ACC, indicating a lack of co-expression with markers of inhibitory interneurons (Figure 1(e) and (f)).

Membrane properties of GRM2-tdtomato and tdtomato-negative ACC neurons from naive mice

Whole-cell patch clamp recordings were performed from 19 *GRM2*-tdtomato and 13 tdtomato-negative layer II/III pyramidal ACC neurons from naive mice (Figure 2(a) and (b); Table 1). A schematic illustrates how measurements were made of action potential properties including threshold, amplitude, tau, and rheobase (Figure 2(c)). For threshold, the action potential waveform voltage was plotted as a derivative, and the value at which membrane voltage increased at a rate of 10 V/s was used. Resting membrane potential between the *GRM2*-tdtomato and tdtomato-negative groups was not different (-65.41 ± 1.55 mV; -65.62 ± 2.33 mV, respectively). However, several measures of membrane excitability were significantly different between *GRM2*-tdtomato and tdtomato-negative subsets, including a significantly less polarized threshold at which action potentials are elicited in the *GRM2*-tdtomato subset (-26.8 mV ± 0.6 mV; -36.4 ± 1.3 mV, respectively), suggesting *GRM2*-tdtomato neurons possess reduced excitability under naive, uninjured conditions compared with tdtomato-negative layer II/III pyramidal ACC neurons. Additionally, *GRM2*-tdtomato neurons exhibited lower action potential peak and more negative AHP voltage, suggesting overall that *GRM2*-tdtomato neurons may be more resistant to activation and produce a less robust signal than tdtomato-negative neurons.

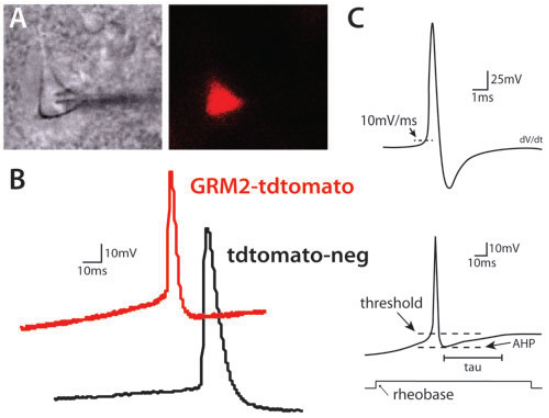

Figure 2. Whole-cell patch-clamp recordings in *GRM2*-tdtomato neurons in ACC. (a) *GRM2*-tdtomato neuron under infrared visualization for patch-clamp recording in adult ACC slice with pipet in view; same cell showing expression of red fluorescent protein. (b) Example traces from typical *GRM2*-tdtomato and tdtomato-negative pyramidal neurons. (c) Schematic for measuring threshold, amplitude, tau, and rheobase. Derivative of voltage curve (above) for measuring the point at which voltage changed by 10 mV/ms which was taken to be threshold at the voltage of the same time point (below). AHP: after-hyperpolarization.

Peripheral inflammation and neuropathic injury enhanced action potential discharge of GRM2-tdtomato ACC neurons

To investigate whether the excitability of *GRM2*-tdtomato layer II/III ACC neurons is altered by peripheral inflammation, 10 µL of CFA was injected subcutaneously into the left plantar hind paw. Coronal brain slices containing ACC were prepared 24 h later from both CFA-injected and naive littermates. A step-current protocol was used to determine the characteristics of evoked responses in *GRM2*-tdtomato ACC neurons. In naive mice, no more than three action potentials were observed in any neuron in response to step current up to the maximum tested, 120 pA (Figure 3(a), top). However, in mice with hind-paw inflammation, 45% of *GRM2*-tdtomato ACC neurons exhibited four or more action potentials during step current (Figure 3(a), bottom, (b)). Therefore, we operationally defined *GRM2*-tdtomato neurons exhibiting four or more action potentials upon a $\leq$120 pA stimulus as "sensitized"; 7 to 10 postoperative days after unilateral chronic constriction injury (CCI) or sham surgery,

Table 1. Membrane properties of *GRM2*-tdtomato and tdtomato-negative neurons from naive mice.

	GRM2-tdtomato (n = 19)	Tdtomato-negative (n = 13)
Resting membrane potential (mV)	-65.41 ± 1.55	-65.62 ± 2.33
Rheobase (pA)	82.63 ± 12.28	52.31 ± 12.31
Threshold (mV)	-26.79 ± 0.57	-36.42 ± 1.34****
AP slope (max, mV/ms)	238.52 ± 34.29	263.35 ± 40.34
AP peak (mV)	66.95 ± 2.26	75.97 ± 2.97*
AP width (ms)	3.3 ± 0.16	4.24 ± 0.55
AHP amplitude (mV)	-41.14 ± 0.89	-48.30 ± 1.63**
Tau (ms)	51.99 ± 5.06	69.37 ± 17.74

AHP: after-hyperpolarization; AP: action potential.

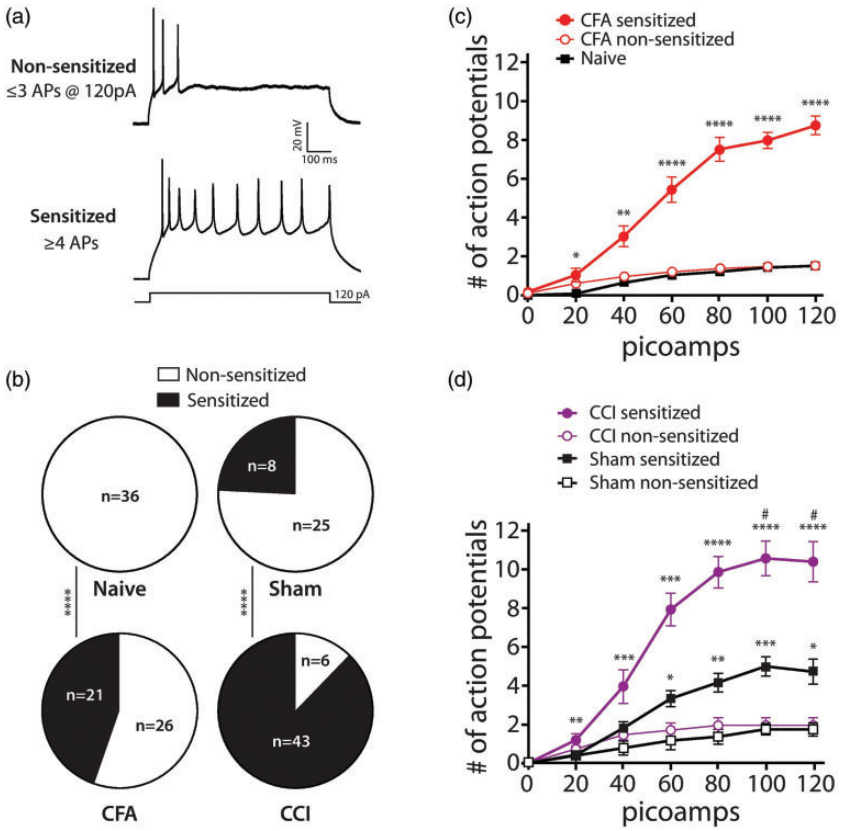

Figure 3. Different proportions of *GRM*2-tdtomato ACC neurons become sensitized depending on injury. (a) A step-current protocol up to 120 pA was run to determine the evoked responses in *GRM*2-tdtomato ACC neurons. Under this protocol, no neurons from naive mice exhibited greater than three action potentials. *GRM*2-tdtomato ACC neurons were therefore defined as sensitized if four or more action potentials were evoked from the treatment groups. (b) Proportion of sensitized neurons from naive, sham, CFA, and CCI treatment groups. Proportion of sensitized versus nonsensitized neurons in naive versus CFA groups was significantly different; as was the proportion between sham and CCI groups (Fisher's exact tests). (c) Number of action potentials evoked from sensitized and nonsensitized naive and CFA across increasing stimulation (two-way repeated measures (RM) ANOVA, Tukey's posttest; * vs. naive). (d) Number of action potentials evoked from sensitized and non-sensitized sham and CCI groups across increasing stimulation (two-way RM ANOVA, Tukey's posttest; * vs. sham nonsensitized; # vs. sham sensitized). AP: action potential; CFA: Complete Freund's Adjuvant; CCI: chronic constriction injury.

whole-cell patch clamp recordings were made from *GRM2*-tdtomato neurons in ACC brain slices. After sham surgery, we observed that 24% of *GRM2*-tdtomato neurons in contralateral ACC met the criteria for sensitized. In the group of mice with CCI, 88% of *GRM2*-tdtomato ACC neurons met the criteria for sensitized (Figure 3(b)). The larger proportion of sensitized neurons after both inflammatory and neuropathic injury versus their respective naive and sham controls was significant (Fisher's exact test, $ps < 0.0001$).

To better characterize the inflammation- and neuropathic-induced sensitization of *GRM2*-tdtomato ACC neurons, increasing stepwise current was delivered while action potential discharge was monitored. Peripheral inflammation of the plantar hind paw with CFA generated increased numbers of action potentials with increasing current in sensitized *GRM2*-tdtomato ACC neurons compared to nonsensitized neurons from CFA-treated mice and neurons from naive mice ($F(2, 71) = 52.36$; $p < 0.0001$) (Figure 3(c)). Likewise, CCI-induced neuropathy generated increased numbers of action potentials in sensitized *GRM2*-tdtomato ACC neurons compared to CCI-nonsensitized, sham-sensitized, and sham nonsensitized groups ($F(3, 34) = 20.70$; $p < 0.0001$) (Figure 3(d)). Consistent with our observation that sham surgery produced a small population of sensitized neurons, stepwise current in sensitized neurons from sham mice produced an enhanced action potential discharge relative to the non-sensitized neurons from sham treated mice (Figure 3(d)). These data together show that *GRM2*-tdtomato ACC neurons from inflammatory and neuropathic injured mice exhibit heightened neural discharge relative to the discharge from naive and sham controls.

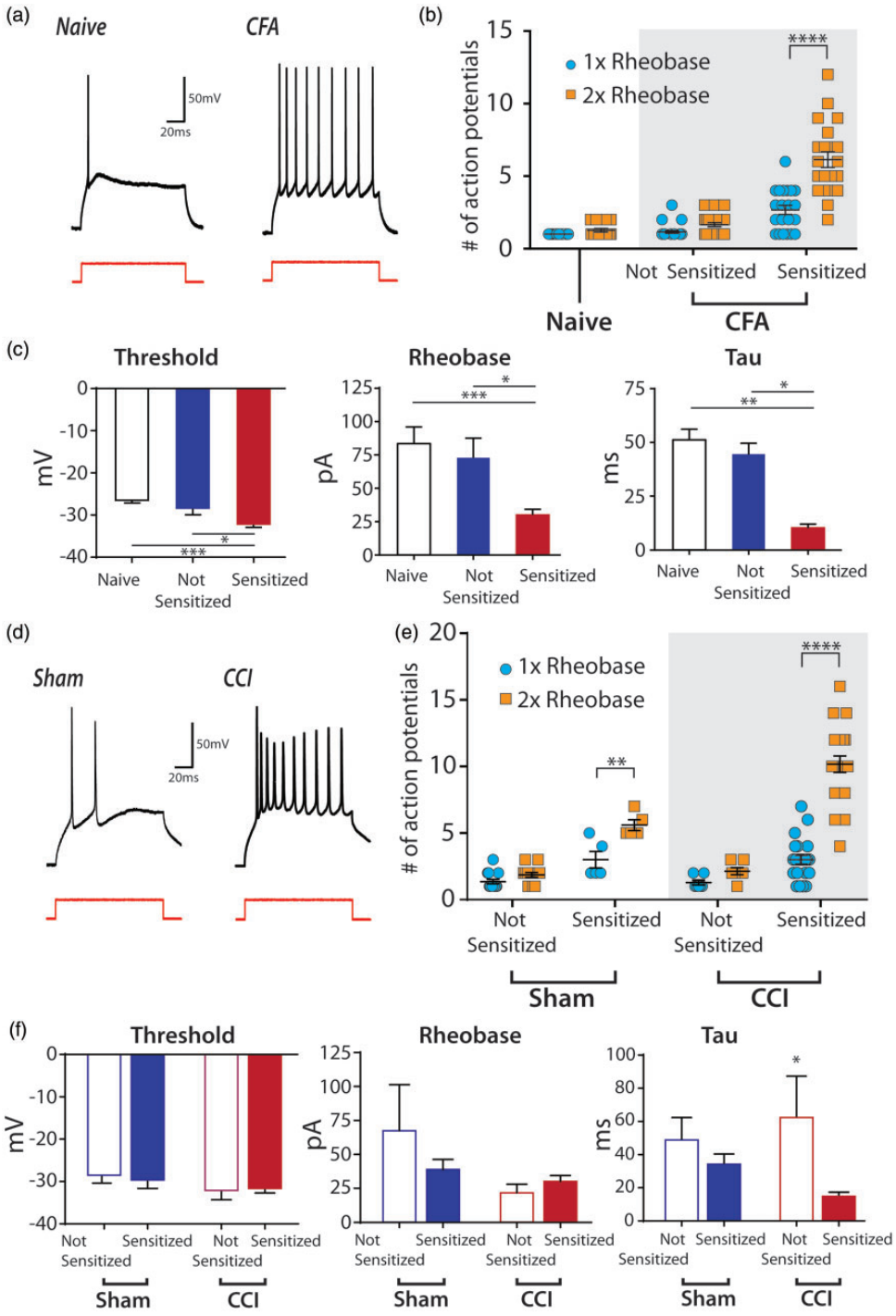

Figure 4. Membrane characteristics of sensitized and nonsensitized *GRM2*-tdtomato ACC neurons in inflammatory and neuropathic treatment groups. (a) Example traces of evoked action potentials in *GRM2*-tdtomato ACC neurons from naive and CFA-treated groups. (b) Comparison of discharge between 1× rheobase and 2× rheobase from sensitized and nonsensitized neurons from naive (n = 19) and CFA (n = 47) groups evoked (two-way ANOVA, Sidak's posttests). (c) Threshold, rheobase, and tau from sensitized and nonsensitized naive and CFA groups (one-way ANOVA with Tukey's posttests. (d) Example traces of evoked action potentials in *GRM2*-tdtomato ACC neurons from sham (n = 12) and CCI-treated (n = 23) groups. (e) Comparison of evoked discharge between 1× rheobase and 2× rheobase from sensitized and nonsensitized neurons from sham and CCI groups (two-way ANOVA, Sidak's posttests). (f) Threshold, rheobase, and tau from sensitized and nonsensitized sham and CCI groups (one-way ANOVA with Tukey's posttests). CFA: Complete Freund's Adjuvant; CCI: chronic constriction injury.

Peripheral and neuropathic injury models increased intrinsic excitability in GRM2-tdtomato ACC neurons

Physiological excitability of *GRM2*-tdtomato ACC neurons from inflammatory and neuropathic mice was further assessed by examining discharge at 1× and 2× rheobase. Examples of typical traces from inflammatory and neuropathic groups are shown (Figure 4(a) and (d)). In nonsensitized neurons from CFA-treated mice, no difference in action potential discharge was observed between 1× and 2× rheobase; however, in sensitized neurons from CFA-treated mice, doubling the rheobase produced a significant increase in action potential discharge ($p < 0.0001$; $F(1, 75) = 22.8$; Figure 4(b)). Similarly, nonsensitized neurons showed no change in discharge of *GRM2*-tdtomato ACC neurons from sham and neuropathic mice at 1× or 2× rheobase, whereas sensitized *GRM2*-tdtomato neurons from sham and CCI groups exhibited significantly greater discharge at 2× compared to 1× rheobase (sham: $p < 0.001$; CCI: $p < 0.0001$; $F(3, 45) = 71.63$; Figure 4(e)). The observed increase in discharge from sensitized neurons from the sham group suggests that sham injury induced neurobiological changes to some neurons in the brain similar to full injury models.

To investigate the cellular biophysical features that could contribute to membrane excitability, rheobase, tau, and AHP were measured in both inflammatory and neuropathic models along with their controls. In the inflammatory model, sensitized neurons exhibited hyperpolarized thresholds, lower rheobase, and shorter tau, relative to the nonsensitized neurons, each of which could contribute to the observed enhanced action potential discharge (Figure 4(c)). AHP voltages were not different between naive (-41.14 ± 0.89 mV), nonsensitized (-42.22 ± 1.19 mV), and sensitized (-43.89 ± 1.05 mV) neuron groups (one-way ANOVA; $p > 0.05$; $F(2, 63) = 1.47$).

Despite the robust action potential discharge evoked from sensitized neurons of neuropathic mice, biophysical membrane properties were largely not different from nonsensitized neurons (Figure 4(d)). Sensitized neurons from the CCI model showed no differences in rheobase or threshold from the nonsensitized neurons within group. Tau was of significantly shorter duration in the sensitized CCI group, similar to what was observed after inflammation (one-way ANOVA; $p < 0.05$; $F(3, 31) = 4.09$). AHP voltage from CCI and sham mice showed that nonsensitized neurons from the CCI group (-43.79 ± 1.87 mV) were significantly hyperpolarized compared to the sham group ($-38.65 \pm$ mV 1.13 mV), one-way ANOVA; $p < 0.05$; $F(2, 32) = 4.14$; Tukey's posttest) but neither were different from the CCI-sensitized group (-40.41 ± 0.76 mV).

Inflammatory and neuropathic hypersensitivity in GRM2-tdtomato ACC neurons was decreased by APDC

To test whether *GRM2*-tdtomato neurons exhibit evidence of functional group II mGluRs, the group II mGluR agonist APDC was bath applied to ACC slices from inflammatory and neuropathic pain models. Previously, 0.5 μM APDC was shown to effectively prevent hyperexcitability in single fiber recordings,[34] and we previously showed that 1 μM APDC prevented hyperexcitability in both human and mouse dissociated dorsal root ganglia when bath applied.[19] In *GRM2*-tdtomato neurons from naive mice, bath application of 1 μM APDC did not change evoked action potential frequency or rheobase (Figure 5(a) to (c)). However, in sensitized *GRM2*-tdtomato ACC neurons from mice with CFA-induced hind-paw inflammation, bath application of APDC increased rheobase (t test, $p < 0.05$) and reduced firing frequency at 2× rheobase (two-way ANOVA $F(1,8) = 8.0$; Sidak's multiple comparison, $p < 0.001$) (Figure 5(d) to (f)). In *GRM2*-tdtomato ACC neurons from mice with CCI neuropathy, APDC likewise increased rheobase (t test, $p < 0.0001$) and reduced firing frequency at 1× and 2× rheobase (two-way ANOVA $F(1, 11) = 53.79$; Sidak's multiple comparison, 1× $p > 0.0001$, 2× $p > 0.05$) (Figure 5(g) to (i)). These data indicate that the *GRM2*-tdtomato neurons possess functional mGluR2 receptors which, when activated, suppress membrane excitability.

Discussion

Group II mGluRs have been implicated as an analgesic target by many studies showing that activation and upregulation of these receptors suppress behavioral responses to nociceptive stimuli.[35–41] Likewise, group II mGluR activation and upregulation suppressed neural responses in dorsal root ganglia and spinal cord neurons, indicating potential sites of action and neural correlates for analgesia.[19,37,42–45] The brain has also been hypothesized as a site for group II mGluRs to modulate pain, in particular within the amygdala and mPFC.[21,46] In a rat model of arthritis, activation of group II mGluRs decreased excitatory synaptic transmission to neurons in the central nucleus of the amygdala and inhibited local action potential discharge.[25,26] Consistent with this, enhancement of group II mGluR activity by the neurotransmitter N-acetylaspartylglutamate in the amygdala reduced excitatory neurotransmission during inflammation.[47] Recently, Mazzitelli and Neugebauer found that group II mGluR activation of the amygdala led to decreased activity in wide dynamic range spinal cord neurons and reduced behavioral indications of pain in rats.[28] Activation of group II mGluRs

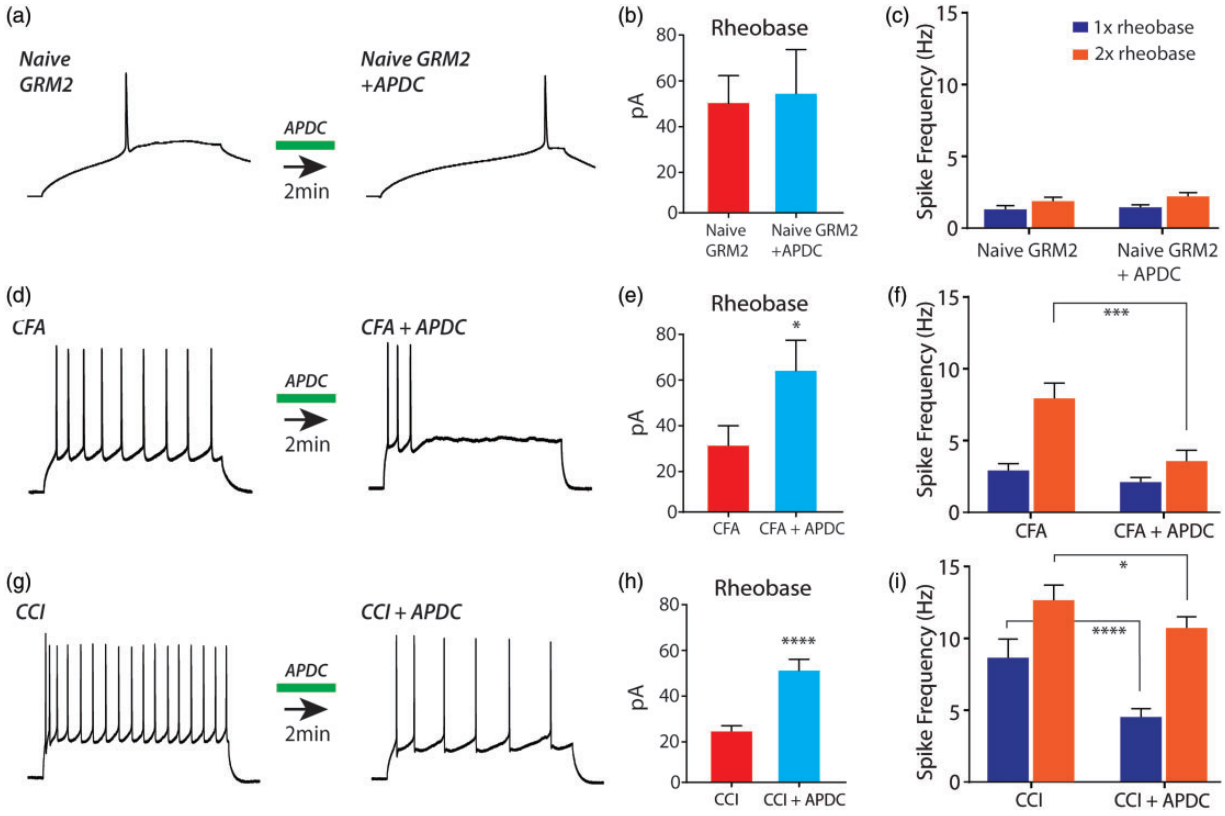

Figure 5. Pharmacological activation of group II mGluRs reduced excitability in *GRM2*-tdtomato ACC neurons from both CFA and CCI models. (a) Example traces of *GRM2*-tdtomato ACC neurons from naive mice. (b) Rheobase and (c) spike discharge at 1× and 2× rheobase were unchanged by bath applied APDC (1 μM). (d) CFA-sensitized *GRM2*-tdtomato ACC neurons displayed fewer action potentials after 2-min treatment with APDC, (e) APDC raised the rheobase ($n = 10$; student's unpaired t test) and (f) decreased the discharge at 2× rheobase (two-way ANOVA, no interaction; main effect of APDC ($p < 0.01$); Sidak's posttests). (g) CCI-sensitized *GRM2*-tdtomato ACC neurons displayed fewer action potentials after 2-min treatment with APDC, (h) APDC raised the rheobase ($n = 24$; student's unpaired t test) and (i) decreased the discharge at 1× and 2× rheobase (two-way ANOVA, no interaction; main effect of APDC ($p < 0.0001$); Sidak's posttests). CFA: Complete Freund's Adjuvant; CCI: chronic constriction injury; APDC: (2R, 4R)-4-Aminopyrrolidine-2,4-dicarboxylate.

also decreased action potential discharge in layer V infralimbic cortex neurons.[27] These studies point to group II mGluRs as targets in multiple brain regions with the capacity to reduce excitability, modulate nociceptive activity, and pain.

In vivo electrophysiological experiments in animal models and human have established that ACC neurons respond to nociceptive stimulation to the body.[33,48–51] The precise contribution of the ACC to the pain experience is under ongoing investigation, but ACC activation during experimentally manipulated negative emotions and the observation of pain in others suggest a multimodal role for the ACC in affective processing of pain and mood.[52–54] Pharmacological evidence shows that modulating Gs-coupled, group I mGluRs in the ACC produce a facilitatory effect on nociceptive withdrawal reflex.[15] Yet knowledge of the function and role of the group II mGluRs in the ACC is limited. Intriguingly, activation of group II mGluRs by oral N-acetylcystein decreased nociceptive electroencephalogram signals from the brain of human subjects, including from within the cingulate region.[55] These observations suggest that different groups of mGluRs in ACC may be positioned to enhance or suppress multiple dimensions of pain-related experience.

Here, we used a novel transgenic reporter mouse to specifically identify and characterize *GRM2* neurons in the ACC using a tdtomato reporter. We evaluated the expression of *GRM2* gene produce in our transgenic tdtomato reporter mice using RNAscope to determine whether tdtomato labeled cells exhibit ongoing expression of *GRM2* and found 78% of tdtomato neurons colocalized with *GRM2* probe. A subset tdtomato cells lacked detectable *GRM2* mRNA colocalization indicating that while these permanently marked cells did not express *GRM2* at the time of testing, they did at some earlier time suggesting that *GRM2* expression in the ACC may be downregulated in some cells. In situ

hybridized label for *GRM2* probe was detected at a number of loci within the ACC without the presence of tdtomato raising the possibility that the transgenic reporter mice used in these studies originating from the Tg(GRM2-cre)MR89Gsat transgenic line had incomplete efficiency. *GRM2*-tdtomato ACC neurons were pyramidal type located in layer II/III possessing an apical dendrite extending to layer I. Immunoreactivity of *GRM2*-tdtomato neurons showed no overlap with parvalbumin or somatostatin, markers typical of cortical inhibitory interneurons. In contrast, these markers were previously found co-expressed with group I mGluRs in several supraspinal areas, supporting the idea that group I and group II mGluRs may be expressed on distinct populations of neurons.[56–58]

Identified *GRM2*-tdtomato and tdtomato-negative pyramidal layer II/III ACC neurons in brain slices were targeted for recording. In the naive animals, *GRM2*-tdtomato ACC neurons displayed a significantly higher action potential threshold, lower action potential peak, and more AHP than tdtomato-negative pyramidal neurons, all of which are indicative of lower basal excitability. We then determined that both peripheral inflammation and neuropathic injury sensitized *GRM2*-tdtomato ACC neurons measured by an increased neuronal discharge upon stimulation. Interestingly, inflammation or neuropathic injury produced different proportions of sensitized *GRM2*-tdtomato ACC neurons, with CCI producing twice the proportion of sensitized neurons compared to CFA. This difference could be related to the duration of the injuries: 24 h for CFA versus 7 to 10 days for CCI; or the extent of body area affected by the injuries: the plantar hind paw for CFA versus more of the hind limb for CCI; or it may reflect the differential regulation of gene expression within nociceptive neurons by inflammatory versus neuropathic models.[59] Altogether, the proportionality suggests a capacity of the ACC to become dynamically engaged based on the quality or magnitude of a specific trauma, as has been previously suggested.[60] This is also consistent with our finding that sham surgery, which involved incision and freeing the nerve, produced a greater proportion of sensitized neurons than observed in naive mice.

The greater capacity for action potential discharge exhibited after either inflammatory or neuropathic injury in *GRM2*-tdtomato ACC neurons may be due in part to changes in intrinsic membrane properties as well as increased excitatory input from presynaptic connections. Sensitized *GRM2*-tdtomato ACC neurons showed no signs of ongoing or spontaneous action potentials after either inflammatory or neuropathic injury, only hypersensitivity in response to stimulation. Interestingly, changes in intrinsic membrane properties, such as rheobase and threshold, suggest a more robust membrane hyperexcitability after inflammation than after CCI, despite a greater overall number of sensitized neurons observed after CCI. We hypothesize that under more chronic pain models, the regulation of hypersensitivity in ACC neurons shifts to become maintained partly from circuit level mechanisms that emerge over time. Consistent with this idea, in vivo recordings after CCI from layer II/III ACC neurons displayed synchrony of subthreshold membrane oscillation that was dependent on local electrical coupling which developed only after seven days postinjury.[61] Synchronized oscillatory could contribute to enhancement of discharge in *GRM2*-tdtomato ACC pyramidal neurons from neuropathic animals upon stimulation or synaptic input from thalamocortical projections.[62]

The ACC receives nociceptive input from midline thalamic nuclei including the centrolateral thalamus and mediodorsal thalamus.[63–65] Previous studies have shown that pain models trigger the development of synaptic plasticity in the ACC.[66–69] Both presynaptic and postsynaptic mechanisms are involved in the onset and maintenance of pain-induced synaptic plasticity in ACC including altered presynaptic transmitter release probability and postsynaptic alpha-amino-3-hydroxy-5-methyl-4-isoxazole propionic acid (AMPA) and N-methyl-D-aspartate (NMDA) receptor density.[11,67,70] In addition to ionotropic glutamate receptors, there is also evidence that functional group I mGluRs contribute to synaptic plasticity in layer II/III ACC.[16] Activation of group I mGluRs could induce long-term depression (LTD) in the ACC and could restore loss of LTD caused by injury.[71] Here, we show that excitability in *GRM2*-tdtomato ACC neurons sensitized after inflammatory and neuropathic injury is suppressed by the group II mGluR agonist APDC. In contrast, naive *GRM2*-tdtomato neurons showed no changes to intrinsic excitability or action potential discharge after bath exposure to APDC. These results indicate the presence of functional group II mGluRs on postsynaptic neurons in ACC that can be targeted selectively during pain, suggesting a pharmacological strategy for regulating excitability of these neurons in vivo.

In summary, *GRM2*-tdtomato pyramidal neurons in layer II/III of the mouse ACC become sensitized by inflammatory and neuropathic injury. These neurons possess functional group II mGluR receptors the activation of which suppressed the increased action potential discharge observed after injury but did not affect membrane properties or discharge under basal conditions. Future studies directed at characterizing the input pathways to *GRM2*-tdtomato ACC neurons as well as their downstream connections will improve our understanding of how these neurons are integrated into nociceptive and emotional circuitry. Drug discovery for mGluRs is an active area of research and clinical trials of mGluR2/3

agonists have already been approved demonstrating a promising safety profile.[21] Therefore, such studies could provide additional mechanistic rationale for the use of group II mGluR agonists and allosteric modulators to treat pain and psychiatric disorders.

Author Contributions

SD conceived of the project; SC, FK, and SD designed the experiments, analyzed the data, and wrote and edited the manuscript; and SC and FK performed the experiments.

Acknowledgments

The authors thank Dr Robert Gereau and Sherri Vogt (Washington University in St. Louis) for the initial generation of the *GRM2*-Cre mice.

Declaration of Conflicting Interests

The author(s) declared no potential conflicts of interest with respect to the research, authorship, and/or publication of this article.

Funding

The author(s) disclosed receipt of the following financial support for the research, authorship, and/or publication of this article: This work was funded by Rita Allen Foundation, Brain and Behavior Foundation, and National Institutes of Health/National Institute of Neurological Disorders and Stroke (NS107356).

ORCID iD

Steve Davidson https://orcid.org/0000-0003-2944-1144

References

1. McWilliams LA, Cox BJ, Enns MW. Mood and anxiety disorders associated with chronic pain: an examination in a nationally representative sample. *Pain* 2003; 106: 127–133.
2. Chapman CR, Tuckett RP, Song CW. Pain and stress in a systems perspective: reciprocal neural, endocrine, and immune interactions. *J Pain* 2008; 9: 122–145.
3. Simons LE, Elman I, Borsook D. Psychological processing in chronic pain: a neural systems approach. *Neurosci Biobehav Rev* 2014; 39: 61–78.
4. Hashmi JA, Baliki MN, Huang L, Baria AT, Torbey S, Hermann KM, Schnitzer TJ, Apkarian AV. Shape shifting pain: chronification of back pain shifts brain representation from nociceptive to emotional circuits. *Brain* 2013; 136: 2751–2768.
5. Cichon J, Blanck TJJ, Gan WB, Yang G. Activation of cortical somatostatin interneurons prevents the development of neuropathic pain. *Nat Neurosci* 2017; 20: 1122–1132.
6. Bushnell MC, Ceko M, Low LA. Cognitive and emotional control of pain and its disruption in chronic pain. *Nat Rev Neurosci* 2013; 14: 502–511.
7. Rainville P, Duncan GH, Price DD, Carrier B, Bushnell MC. Pain affect encoded in human anterior cingulate but not somatosensory cortex. *Science* 1997; 277: 968–971.
8. May A. Chronic pain may change the structure of the brain. *Pain* 2008; 137: 7–15.
9. Shackman AJ, Salomons TV, Slagter HA, Fox AS, Winter JJ, Davidson RJ. The integration of negative affect, pain and cognitive control in the cingulate cortex. *Nat Rev Neurosci* 2011; 12: 154–167.
10. Baliki MN, Apkarian AV. Nociception, pain, negative moods, and behavior selection. *Neuron* 2015; 87: 474–491.
11. Bliss TV, Collingridge GL, Kaang BK, Zhuo M. Synaptic plasticity in the anterior cingulate cortex in acute and chronic pain. *Nat Rev Neurosci* 2016; 17: 485–496.
12. Yan N, Cao B, Xu J, Hao C, Zhang X, Li Y. Glutamatergic activation of anterior cingulate cortex mediates the affective component of visceral pain memory in rats. *Neurobiol Learn Mem* 2012; 97: 156–164.
13. Li W, Wang P, Li H. Upregulation of glutamatergic transmission in anterior cingulate cortex in the diabetic rats with neuropathic pain. *Neurosci Lett* 2014; 568: 29–34.
14. Mussio CA, Harte SE, Borszcz GS. Regional differences within the anterior cingulate cortex in the generation versus suppression of pain affect in rats. *J Pain*. Epub ahead of print 16 June 2019. DOI: 10.1016/j.jpain.2019.06.003.
15. Calejesan AA, Kim SJ, Zhuo M. Descending facilitatory modulation of a behavioral nociceptive response by stimulation in the adult rat anterior cingulate cortex. *Eur J Pain* 2000; 4: 83–96.
16. Koga K, Li S, Zhuo M. Metabotropic glutamate receptor dependent cortical plasticity in chronic pain. *Curr Neuropharmacol* 2016; 14: 427–434.
17. Guo B, Wang J, Yao H, Ren K, Chen J, Yang J, Cai G, Liu H, Fan Y, Wang W, Wu S. Chronic Inflammatory pain impairs mGluR5-mediated depolarization-induced suppression of excitation in the anterior cingulate cortex. *Cereb Cortex* 2018; 28: 2118–2130.
18. Gereau RW, Swanson G. *The glutamate receptors*. Totowa: Humana Press, 2008.
19. Davidson S, Golden JP, Copits BA, Ray PR, Vogt SK, Valtcheva MV, Schmidt RE, Ghetti A, Price TJ, Gereau RW. Group II mGluRs suppress hyperexcitability in mouse and human nociceptors. *Pain* 2016; 157: 2081–2088.
20. Gu G, Lorrain DS, Wei H, Cole RL, Zhang X, Daggett LP, Schaffhauser HJ, Bristow LJ, Lechner SM. Distribution of metabotropic glutamate 2 and 3 receptors in the rat forebrain: implication in emotional responses and central disinhibition. *Brain Res* 2008; 1197: 47–62.
21. Mazzitelli M, Palazzo E, Maione S, Neugebauer V. Group II metabotropic glutamate receptors: role in pain mechanisms and pain modulation. *Front Mol Neurosci* 2018; 11: 383.
22. Venkatadri PS, Lee CC. Differential expression of mGluR2 in the developing cerebral cortex of the mouse. *J Biomed Sci Eng* 2014; 7: 1030–1037.
23. Montana MC, Gereau RW. Metabotropic glutamate receptors as targets for analgesia: antagonism, activation,

and allosteric modulation. *Curr Pharm Biotechnol* 2011; 12: 1681–1688.
24. Johnson MP, Muhlhauser MA, Nisenbaum ES, Simmons RMA, Forster BM, Knopp KL, Yang L, Morrow D, Li DL, Kennedy JD, Swanson S, Monn J A. Broad spectrum efficacy with LY2969822, an oral prodrug of metabotropic glutamate 2/3 receptor agonist LY2934747, in rodent pain models. *Br J Pharmacol* 2017; 174: 822–835.
25. Han JS, Fu Y, Bird GC, Neugebauer V. Enhanced group II mGluR-mediated inhibition of pain-related synaptic plasticity in the amygdala. *Mol Pain* 2006; 2: 18.
26. Li W, Neugebauer V. Differential changes of group II and group III mGluR function in central amygdala neurons in a model of arthritic pain. *J Neurophysiol* 2006; 96: 1803–1815.
27. Kiritoshi T, Neugebauer V. Group II mGluRs modulate baseline and arthritis pain-related synaptic transmission in the rat medial prefrontal cortex. *Neuropharmacology* 2015; 95: 388–394.
28. Mazzitelli M, Neugebauer V. Amygdala group II mGluRs mediate the inhibitory effects of systemic group II mGluR activation on behavior and spinal neurons in a rat model of arthritis pain. *Neuropharmacology* 2019; 158: 107706.
29. Bocchio M, Lukacs IP, Stacey R, Plaha P, Apostolopoulos V, Livermore L, Sen A, Ansorge O, Gillies MJ, Somogyi P, Capogna M. Group II metabotropic glutamate receptors mediate presynaptic inhibition of excitatory transmission in pyramidal neurons of the human cerebral cortex. *Front Cell Neurosci* 2018; 12: 508.
30. O'Brien DE, Alter BJ, Satomoto M, Morgan CD, Davidson S, Vogt SK, Norman ME, Gereau GB, Demaro JA, Landreth GE, Golden JP, Gereau RW. ERK2 alone drives inflammatory pain but cooperates with ERK1 in sensory neuron survival. *J Neurosci* 2015; 35: 9491–9507.
31. Bennett GJ, Xie YK. A peripheral mononeuropathy in rat that produces disorders of pain sensation like those seen in man. *Pain* 1988; 33: 87–107.
32. Ohishi H, Neki A, Mizuno N. Distribution of a metabotropic glutamate receptor, mGluR2, in the central nervous system of the rat and mouse: an immunohistochemical study with a monoclonal antibody. *Neurosci Res* 1998; 30: 65–82.
33. Shyu BC, Sikes RW, Vogt LJ, Vogt BA. Nociceptive processing by anterior cingulate pyramidal neurons. *J Neurophysiol* 2010; 103: 3287–3301.
34. Du J, Zhou S, Carlton SM. Group II metabotropic glutamate receptor activation attenuates peripheral sensitization in inflammatory states. *Neuroscience* 2008; 154: 754–766.
35. Sharpe EF, Kingston AE, Lodge D, Monn JA, Headley PM. Systemic pre-treatment with a group II mGlu agonist, LY379268, reduces hyperalgesia in vivo. *Br J Pharmacol* 2002; 135: 1255–1262.
36. Simmons RM, Webster AA, Kalra AB, Iyengar S. Group II mGluR receptor agonists are effective in persistent and neuropathic pain models in rats. *Pharmacol Biochem Behav* 2002; 73: 419–427.
37. Yang D, Gereau RWt. Peripheral group II metabotropic glutamate receptors mediate endogenous anti-allodynia in inflammation. *Pain* 2003; 106: 411–417.
38. Zammataro M, Chiechio S, Montana MC, Traficante A, Copani A, Nicoletti F, Gereau RW. mGlu2 metabotropic glutamate receptors restrain inflammatory pain and mediate the analgesic activity of dual mGlu2/mGlu3 receptor agonists. *Mol Pain* 2011; 7: 6.
39. Zammataro M, Sortino MA, Parenti C, Gereau RW, Chiechio S. HDAC and HAT inhibitors differently affect analgesia mediated by group II metabotropic glutamate receptors. *Mol Pain* 2014; 10: 68.
40. Cao DY, Bai G, Ji Y, Traub RJ. Epigenetic upregulation of metabotropic glutamate receptor 2 in the spinal cord attenuates oestrogen-induced visceral hypersensitivity. *Gut* 2015; 64: 1913–1920.
41. Cao DY, Bai G, Ji Y, Karpowicz JM, Traub RJ. EXPRESS: histone hyperacetylation modulates spinal type II metabotropic glutamate receptor alleviating stress-induced visceral hypersensitivity in female rats. *Mol Pain* 2016; 12: 174480691666072–174480691666008.
42. Neugebauer V, Chen PS, Willis WD. Groups II and III metabotropic glutamate receptors differentially modulate brief and prolonged nociception in primate STT cells. *J Neurophysiol* 2000; 84: 2998–3009.
43. Carlton SM, Du J, Zhou S. Group II metabotropic glutamate receptor activation on peripheral nociceptors modulates TRPV1 function. *Brain Res* 2009; 1248: 86–95.
44. Carlton SM, Zhou S, Govea R, Du J. Group II/III metabotropic glutamate receptors exert endogenous activity-dependent modulation of TRPV1 receptors on peripheral nociceptors. *J Neurosci* 2011; 31: 12727–12737.
45. Sheahan TD, Valtcheva MV, McIlvried LA, Pullen MY, Baranger DAA, Gereau RWt. Metabotropic glutamate receptor 2/3 (mGluR2/3) activation suppresses TRPV1 sensitization in mouse, but not human, sensory neurons. *eNeuro* 2018; 5: ENEURO.0412-17.2018.
46. Chiechio S. Modulation of chronic pain by metabotropic glutamate receptors. *Adv Pharmacol* 2016; 75: 63–89.
47. Adedoyin MO, Vicini S, Neale JH. Endogenous N-acetylaspartylglutamate (NAAG) inhibits synaptic plasticity/transmission in the amygdala in a mouse inflammatory pain model. *Mol Pain* 2010; 6: 60.
48. Hutchison WD, Davis KD, Lozano AM, Tasker RR, Dostrovsky JO. Pain-related neurons in the human cingulate cortex. *Nat Neurosci* 1999; 2: 403–405.
49. Sikes RW, Vogt LJ, Vogt BA. Distribution and properties of visceral nociceptive neurons in rabbit cingulate cortex. *Pain* 2008; 135: 160–174.
50. Kuo CC, Yen CT. Comparison of anterior cingulate and primary somatosensory neuronal responses to noxious laser-heat stimuli in conscious, behaving rats. *J Neurophysiol* 2005; 94: 1825–1836.
51. Iwata K, Kamo H, Ogawa A, Tsuboi Y, Noma N, Mitsuhashi Y, Taira M, Koshikawa N, Kitagawa J. Anterior cingulate cortical neuronal activity during perception of noxious thermal stimuli in monkeys. *J Neurophysiol* 2005; 94: 1980–1991.
52. Singer T, Seymour B, O'Doherty J, Kaube H, Dolan RJ, Frith CD. Empathy for pain involves the affective but not sensory components of pain. *Science* 2004; 303: 1157–1162.

53. Wiech K, Tracey I. The influence of negative emotions on pain: behavioral effects and neural mechanisms. *Neuroimage* 2009; 47: 987–994.
54. Zaki J, Wager TD, Singer T, Keysers C, Gazzola V. The anatomy of suffering: understanding the relationship between nociceptive and empathic pain. *Trends Cogn Sci (Regul Ed)* 2016; 20: 249–259.
55. Truini A, Piroso S, Pasquale E, Notartomaso S, Di Stefano G, Lattanzi R, Battaglia G, Nicoletti F, Cruccu G. N-acetyl-cysteine, a drug that enhances the endogenous activation of group-II metabotropic glutamate receptors, inhibits nociceptive transmission in humans. *Mol Pain* 2015; 11: 14.
56. Kocsis K, Kiss J, Gorcs T, Halasz B. Metabotropic glutamate receptor in vasopressin, CRF and VIP hypothalamic neurones. *Neuroreport* 1998; 9: 4029–4033.
57. van Hooft JA, Giuffrida R, Blatow M, Monyer H. Differential expression of group I metabotropic glutamate receptors in functionally distinct hippocampal interneurons. *J Neurosci* 2000; 20: 3544–3551.
58. Barnes SA, Pinto-Duarte A, Kappe A, Zembrzycki A, Metzler A, Mukamel EA, Lucero J, Wang X, Sejnowski TJ, Markou A, Behrens MM. Disruption of mGluR5 in parvalbumin-positive interneurons induces core features of neurodevelopmental disorders. *Mol Psychiatry* 2015; 20: 1161–1172.
59. LaCroix-Fralish ML, Austin JS, Zheng FY, Levitin DJ, Mogil JS. Patterns of pain: meta-analysis of microarray studies of pain. *Pain* 2011; 152: 1888–1898.
60. Zhang Y, Wang N, Wang JY, Chang JY, Woodward DJ, Luo F. Ensemble encoding of nociceptive stimulus intensity in the rat medial and lateral pain systems. *Mol Pain* 2011; 7: 64.
61. Chen Z, Shen X, Huang L, Wu H, Zhang M. Membrane potential synchrony of neurons in anterior cingulate cortex plays a pivotal role in generation of neuropathic pain. *Sci Rep* 2018; 8: 1691.
62. Shih HC, Yang JW, Lee CM, Shyu BC. Spontaneous cingulate high-current spikes signal normal and pathological pain states. *J Neurosci* 2019; 39: 5128–5142.
63. Yang JW, Shih HC, Shyu BC. Intracortical circuits in rat anterior cingulate cortex are activated by nociceptive inputs mediated by medial thalamus. *J Neurophysiol* 2006; 96: 3409–3422.
64. Shyu BC, Vogt BA. Short-term synaptic plasticity in the nociceptive thalamic-anterior cingulate pathway. *Mol Pain* 2009; 5: 51.
65. Delevich K, Tucciarone J, Huang ZJ, Li B. The mediodorsal thalamus drives feedforward inhibition in the anterior cingulate cortex via parvalbumin interneurons. *J Neurosci* 2015; 35: 5743–5753.
66. Xu H, Wu L-J, Wang H, Zhang X, Vadakkan KI, Kim SS, Steenland HW, Zhuo M. Presynaptic and postsynaptic amplifications of neuropathic pain in the anterior cingulate cortex. *J Neurosci* 2008; 28: 7445–7453.
67. Toyoda H, Zhao MG, Zhuo M. Enhanced quantal release of excitatory transmitter in anterior cingulate cortex of adult mice with chronic pain. *Mol Pain* 2009; 5: 4.
68. Li X-Y, Ko H-G, Chen T, Descalzi G, Koga K, Wang H, Kim SS, Shang Y, Kwak C, Park S-W, Shim J, Lee K, Collingridge GL, Kaang B-K, Zhuo M. Alleviating neuropathic pain hypersensitivity by inhibiting PKMzeta in the anterior cingulate cortex. *Science* 2010; 330: 1400–1404.
69. Chen T, Wang W, Dong Y-L, Zhang M-M, Wang J, Koga K, Liao Y-H, Li J-L, Budisantoso T, Shigemoto R, Itakura M, Huganir RL, Li Y-Q, Zhuo M. Postsynaptic insertion of AMPA receptor onto cortical pyramidal neurons in the anterior cingulate cortex after peripheral nerve injury. *Mol Brain* 2014; 7: 76.
70. Wu LJ, Li X, Chen T, Ren M, Zhuo M. Characterization of intracortical synaptic connections in the mouse anterior cingulate cortex using dual patch clamp recording. *Mol Brain* 2009; 2: 32.
71. Kang SJ, Liu M-G, Chen T, Ko H-G, Baek G-C, Lee H-R, Lee K, Collingridge GL, Kaang B-K, Zhuo M. Plasticity of metabotropic glutamate receptor-dependent long-term depression in the anterior cingulate cortex after amputation. *J Neurosci* 2012; 32: 11318–11329.